TWO COUNTEREXAMPLES TO A CONJECTURE OF COLIN DE VERDIÈRE ON MULTIPLICITY

MAXIME FORTIER BOURQUE, ÉMILE GRUDA-MEDIAVILLA, BRAM PETRI, AND MATHIEU PINEAULT

Abstract. We exhibit closed hyperbolic surfaces of genus 10 and 17 such that the multiplicity of the first nonzero eigenvalue of their Laplacian is larger than the maximum conjectured by Yves Colin de Verdière in 1986. In order to determine these multiplicities, we apply the twisted Selberg trace formula to the representations induced by the isometry groups of these surfaces on corresponding triangle groups.

1. Introduction

Let Σ be a closed, connected, smooth manifold of dimension at least 1. For a Riemannian metric h on Σ, let $\lambda_1(\Sigma, h)$ be the smallest nonzero eigenvalue of the Laplacian with respect to h acting on smooth real-valued functions on Σ and let $m_1(\Sigma, h)$ be its multiplicity, that is, the dimension of the corresponding eigenspace. Furthermore, consider

$$\overline{m}_1(\Sigma) := \sup\{m_1(\Sigma, h) : h \text{ is a Riemannian metric on } \Sigma\}.$$

In [CdV86] and [CdV87], Colin de Verdière conjectured that $\overline{m}_1(\Sigma) = \operatorname{chr}(\Sigma) - 1$, where the *chromatic number* $\operatorname{chr}(\Sigma)$ is defined as the supremum of the natural numbers n such that the complete graph on n vertices embeds in Σ. By results from [Hea90], [RY68], and [AH77, AHK77], every finite graph embeddable in a surface Σ can be colored with at most $\operatorname{chr}(\Sigma)$ colors so that adjacent vertices have different colors, hence the name.

Colin de Verdière's conjecture is true if $\dim(\Sigma) = 1$, if $\dim(\Sigma) \geq 3$ [CdV86], or if Σ is the 2-sphere [Che76], the 2-torus [Bes80], the projective plane [Bes80], or the Klein bottle [CdV87, Nad87]. Many efforts were made to try to prove the conjecture in general [Bes87, Sév02, LM23], but to no avail. We will show that the conjecture is in fact false.

Theorem 1.1. *There exist closed, connected, orientable, hyperbolic surfaces X_{10} and X_{17}, of genus 10 and 17 respectively, satisfying $m_1(X_{10}) = 16 > 13 = \operatorname{chr}(X_{10}) - 1$ and $m_1(X_{17}) = 21 > 16 = \operatorname{chr}(X_{17}) - 1$.*

Note that the chromatic number of a closed connected surface Σ different from the Klein bottle is $\left\lfloor \frac{1}{2}\left(7 + \sqrt{49 - 24\chi(\Sigma)}\right)\right\rfloor$ by a result of Ringel and Youngs [RY68], where χ is the Euler characteristic. The chromatic number of the Klein bottle is equal to 6 rather than 7. In particular, if Σ is orientable of genus g, then its chromatic number is equal to $\left\lfloor \frac{1}{2}\left(7 + \sqrt{48g+1}\right)\right\rfloor$, which yields the right-hand side equalities in Theorem 1.1.

Date: December 21, 2023.

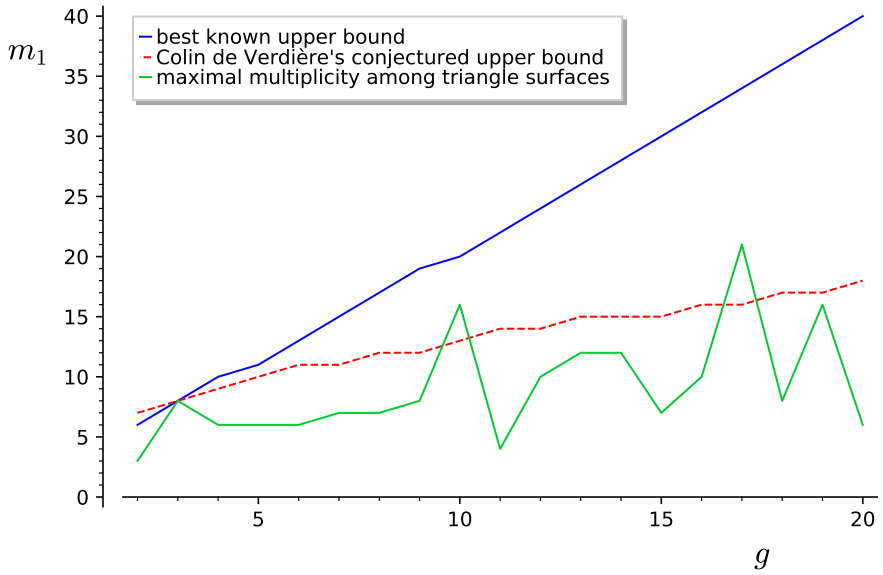

FIGURE 1. Upper and lower bounds on the largest multiplicity among hyperbolic surfaces of genus g between 2 and 20. The green curve is based on numerical results that have been verified rigorously in genus 2 and 3 [FBP23a], 7 [Lee23], 10 and 17 (present paper).

The surfaces X_{10} and X_{17} in Theorem 1.1 are $(2,3,8)$- and $(2,3,7)$-triangle surfaces which happen to be normal covers of the Bolza and Klein surfaces in genus 2 and 3, respectively. They were discovered by Émile Gruda-Mediavilla with the help of Mathieu Pineault during a summer research project supervised by Maxime Fortier Bourque. The goal of the project was to compute λ_1 and m_1 numerically for all triangle surfaces of genus 2 to 20 using the computer program `FreeFEM++`. The largest approximate multiplicity we found in each genus is shown in Figure 1 together with Colin de Verdière's conjectured maximum and the upper bound from [FBP23b] (valid for hyperbolic surfaces only).

1.1. **Outline of proof.** We now describe how we prove that $m_1(X_{10})$ and $m_1(X_{17})$ are as large as observed numerically. These techniques will be applied in a forthcoming paper to confirm the remaining multiplicities in Figure 1. In [FBP23a], it was shown that the Bolza surface B and the Klein quartic K satisfy $m_1(B) = 3$ and $m_1(K) = 8$ using the representation theory of their isometry groups and the Selberg trace formula. The idea is that the eigenspaces of the Laplacian can be decomposed into direct sums of irreducible representations (irreps) of the isometry group (or any of its subgroups). If the irreducible representations of small dimension can be ruled out from appearing in the eigenspace corresponding to λ_1, that forces m_1 to be large. The proof of Theorem 1.1 is based on the same general idea but uses improved methods to exclude representations.

The surfaces X_{10} and X_{17} happen to be chiral, meaning that all their isometries are orientation-preserving. The dimensions of the irreducible representations of $\mathrm{Isom}^+(X_{10})$ and $\mathrm{Isom}^+(X_{17})$ over $\mathbb{R}$ are

$$1, 1, 2, 3, 3, 4, 4, 4, 8, 8, 16 \quad \text{and} \quad 1, 6, 6, 6, 7, 7, 7, 8, 14, 21, 21$$

(see Appendix A) while the corresponding dimensions for $\mathrm{Isom}^+(B)$ and $\mathrm{Isom}^+(K)$ are

$$1, 1, 2, 3, 3, 4, 4, 4 \quad \text{and} \quad 1, 6, 6, 6, 7, 8.$$

There is a reason why the second lists are subsets of the first. Since the covers $X_{10} \to B$ and $X_{17} \to K$ are normal, they induce homomorphisms between the groups of orientation-preserving isometries, and therefore any irreducible representation for the base surface gives rise to an irreducible representation of the same dimension for the cover. Moreover, the eigenfunctions appearing in these induced representations are simply lifts of eigenfunctions on the base surface, hence they correspond to the same eigenvalue. Any non-trivial eigenvalue of X_{10} or X_{17} coming from such induced representations must therefore be at least as large as $\lambda_1(B) \approx 3.838$ or $\lambda_1(K) \approx 2.678$ respectively. However, previous upper bounds from [FBP23b, Table 3] imply that $\lambda_1(X_{10}) \leq 1.223$ and $\lambda_1(X_{17}) \leq 0.969$. Hence, this already rules out most of the irreducible representations from appearing in the first eigenspace. For X_{10} there are only two irreps of dimension 8 left to exclude and for X_{17} there are two of dimension 7 and one of dimension 14.

How does one rule out these additional irreps? In [FBP23a] and [FBP23b], Courant's nodal theorem was used to exclude 1-dimensional irreps under certain conditions and some ad hoc methods were used to exclude 2-dimensional irreps for the Bolza surface, following [Coo18] and [Jen81]. The Selberg trace formula was also used to prove bounds on the number of eigenvalues in certain intervals for the Klein quartic, yielding the result that $m_1(K) = 8$. However, this method would not work here since there could be two nearby eigenvalues whose multiplicities add up to $16 = 8 + 8$ or $21 = 7 + 14$.

The additional ingredient required is the *twisted* Selberg trace formula. This version of the trace formula yields information on the eigenvalues associated with individual representations of the isometry group. By applying it to the irreducible representations of non-maximal dimension with suitable test functions, we show that the corresponding eigenvalues are strictly larger than the first positive eigenvalue of the surface. This implies that $m_1(X_{10}) \geq 16$ and $m_1(X_{17}) \geq 21$, and previous upper bounds on multiplicity imply that equality holds in both cases. Note that this method rules out all the irreducible representations except the top-dimensional ones, so we do not even need the above argument regarding the representations induced by the Bolza and Klein surfaces in the end.

1.2. **Notes and comments.** We conclude the introduction by pointing out that although Colin de Verdière's conjecture turns out to be false, it would be interesting to know if it is asymptotically true. In particular, is it true that $\overline{m}_1(\Sigma) = O(\sqrt{|\chi(\Sigma)|} + 1)$?

The best known constructions [BC85, CCdV88] achieve this rate of growth with hyperbolic surfaces. To achieve higher multiplicity than in [BC85] using representation theory, one would need to build regular covers of a base orbifold where several large-dimensional irreps of the deck group are forced to appear together in the first eigenspace. Just one irrep is not enough because their dimension is bounded by the square root of the cardinality of the group, which is proportional to the Euler characteristic.

The best known upper bound on $\overline{m}_1$ without restrictions on the metric when $\chi(\Sigma) < 0$ is $5 - \chi(\Sigma)$ [Sév02]. This was improved to $2g - 1$ for hyperbolic surfaces of large enough

genus g in [FBP23b] and a sublinear upper bound was obtained in [LM23] for pinched negatively curved surfaces with injectivity radius bounded away from zero.

Acknowledgements. We thank the `FreeFEM++` [Hec12], `SageMath` [The21], `Arb` [Joh17], and `GAP` [GAP22] developers for making the calculations in this paper possible.

Funding. MFB was partially supported by a Discovery Grant from the Natural Sciences and Engineering Research Council of Canada (NSERC), EGM was supported by an Undergraduate Student Research Award from NSERC, and MP was supported by a Master's Training Scholarship from the Fonds de Recherche du Québec Nature et Technologies and a Canada Graduate Scholarship from NSERC.

2. Spectral theory of co-compact Fuchsian groups

In this section, we review some of the spectral theory of cocompact Fuchsian groups. Our discussion is mostly based on [Hej76] and [CP23], to which we refer for details and a more complete overiew. Our standing assumptions will be:

- $\Gamma < \mathrm{PSL}(2,\mathbb{R})$ is a co-compact (but not necessarily torsion-free) Fuchsian group,
- $\Lambda < \Gamma$ is a normal subgroup of finite index,
- $G = \Gamma/\Lambda$ is the quotient group,
- $\rho : \Gamma \to G$ is the quotient map.

These hypotheses imply that there is a normal branched cover $\Lambda\backslash\mathbb{H}^2 \to \Gamma\backslash\mathbb{H}^2$ with deck group G. In the cases that interest us, $\Lambda\backslash\mathbb{H}^2$ will be a triangle surface, G its group of orientation-preserving isometries, and Γ the corresponding triangle group, so that the quotient $\Gamma\backslash\mathbb{H}^2$ is the double of a hyperbolic triangle across its boundary.

We also let $\mathbb{F}$ be either $\mathbb{R}$ or $\mathbb{C}$. Usually, the Laplacian is taken to act on real-valued functions, but the definition extends to complex-valued functions by linearity. It is more natural to use $\mathbb{R}$ in spectral geometry, but more convenient to use $\mathbb{C}$ in representation theory.

2.1. Twisted Laplacians.

Let $C^\infty(\Lambda\backslash\mathbb{H}^2)$ be the space of smooth $\mathbb{F}$-valued Λ-invariant functions on $\mathbb{H}^2$, let Δ be the Laplacian acting on such functions, and let $\mathrm{spec}(\Lambda\backslash\mathbb{H}^2)$ denote the spectrum of Δ as a multiset, where eigenvalues are listed with multiplicity.

The group G acts on $\Lambda\backslash\mathbb{H}^2$ by isometries so that the induced action on $C^\infty(\Lambda\backslash\mathbb{H}^2)$ by precomposition commutes with the Laplacian. This implies that the eigenspaces of the Laplacian can be decomposed into irreducible representations of G. We will describe this decomposition using twisted Laplacians. Since the quotient of $\Lambda\backslash\mathbb{H}^2$ by G is $\Gamma\backslash\mathbb{H}^2$, the objects in question will be defined over that smaller quotient.

Let V be a finite-dimensional vector space over $\mathbb{F}$ equipped with a Hermitian inner product and let $\varphi : \Gamma \to \mathrm{GL}(V)$ be a unitary representation. We write $C^\infty(\Gamma\backslash\mathbb{H}^2, \varphi)$ for the space of smooth functions $F : \mathbb{H}^2 \to V$ such that

$$F(\gamma(z)) = \varphi(\gamma)(F(z)), \quad \text{for all } z \in \mathbb{H}^2 \text{ and all } \gamma \in \Gamma.$$

We can extend the definition of the Laplacian to $C^\infty(\Gamma\backslash\mathbb{H}^2,\varphi)$ by making it act coordinate-wise with respect to an orthonormal basis for V and this *twisted Laplacian* is denoted by Δ_φ. The hypothesis that φ is unitary is used so that $\varphi(\gamma)$ is an isometry, hence commutes with Δ_φ, so that $\Delta_\varphi F$ satisfies the same equivariance property as F, i.e., belongs to $C^\infty(\Gamma\backslash\mathbb{H}^2,\varphi)$ as well. We write $\mathrm{spec}(\Gamma\backslash\mathbb{H}^2,\varphi)$ for the spectrum of Δ_φ.

If $\varphi=\phi\circ\rho$ is induced by a unitary representation $\phi: G\to \mathrm{GL}(V)$ via the quotient map $\rho:\Gamma\to G$, then we write $\mathrm{spec}(\Gamma\backslash\mathbb{H}^2,\phi)$ instead of $\mathrm{spec}(\Gamma\backslash\mathbb{H}^2,\varphi)$.

2.2. **The decomposition.** Let $\mathrm{Irr}(G)$ be the set of (equivalence classes of) irreducible representations of G over $\mathbb{F}$, chosen to be unitary (which is always possible by Weyl's trick). The decomposition of $\mathrm{spec}(\Lambda\backslash\mathbb{H}^2)$ into irreducible representations of G can be written as follows.

Proposition 2.1. *If $\Lambda<\Gamma$ are co-compact Fuchsian groups and $G=\Gamma/\Lambda$ is finite, then*

$$\mathrm{spec}(\Lambda\backslash\mathbb{H}^2)=\bigcup_{\phi\in\mathrm{Irr}(G)}\dim_{\mathbb{F}}(\phi)\cdot\mathrm{spec}(\Gamma\backslash\mathbb{H}^2,\phi)$$

as multisets.

Here, multiplying a multiset by d means multiplying the multiplicities by d. For a proof of this proposition, see for instance [CP23, Sections 3.8 and 3.9]. Technically, our set-up is slightly different from that of Cornelissen and Peyerimhoff: they consider the spectrum of the Laplacian on a Riemannian manifold. However, their proof goes through for orbifolds as well. The only minor difference is how the spaces $C^\infty(\Lambda\backslash\mathbb{H}^2)$ and $C^\infty(\Gamma\backslash\mathbb{H}^2,\varphi)$ are defined.

2.3. **The twisted Selberg trace formula.** In order to access the spectra appearing on the right-hand side of Proposition 2.1, we will use the twisted Selberg trace formula. To state it, we need some further notation.

Given an integrable function $f:\mathbb{R}\to\mathbb{C}$, its Fourier transform $\widehat{f}$ is given by

$$\widehat{f}(y)=\int_{-\infty}^{\infty}f(x)\,e^{-iy\cdot x}\,dx.$$

We will call f *admissible* if it is even and there exists an $\varepsilon>0$ such that $\widehat{f}$ is holomorphic on a strip $\mathcal{S}_\varepsilon=\{z\in\mathbb{C};\ |\mathrm{Im}(z)|<\frac{1}{2}+\varepsilon\}$ and

$$\widehat{f}(y)=O\left((1+|y|)^{-2-\varepsilon}\right)$$

in $\mathcal{S}_\varepsilon$.

If $\Gamma<\mathrm{PSL}(2,\mathbb{R})$ is a cocompact Fuchsian group, $\varphi:\Gamma\to\mathrm{GL}(V)$ is a finite-dimensional unitary representation, and f is an admissible function, then the *twisted Selberg trace*

formula (see [Hej76, p. 351]) states that

$$\sum_{\lambda\in\mathrm{spec}(\Gamma\backslash\mathbb{H}^2,\varphi)} \widehat{f}\left(\sqrt{\lambda-\frac{1}{4}}\right) = \dim(\varphi)\frac{\mathrm{area}(\Gamma\backslash\mathbb{H}^2)}{4\pi}\int_{-\infty}^{\infty} y\widehat{f}(y)\tanh(\pi y)\,dy + \sum_{[\gamma]\in\mathcal{E}(\Gamma)} \frac{\mathrm{tr}\,(\varphi(\gamma))}{2m(\gamma)\sin(\theta(\gamma))}\int_{-\infty}^{\infty}\frac{e^{-2\theta(\gamma)y}}{1+e^{-2\pi y}}\widehat{f}(y)\,dy + \sum_{[\gamma]\in\mathcal{P}(\Gamma)} \ell(\gamma)\sum_{n\geq 1}\frac{\mathrm{tr}\,(\varphi(\gamma^n))}{2\sinh(n\ell(\gamma)/2)}f(n\ell(\gamma)) \tag{2.1}$$

Here,

- $\mathcal{E}(\Gamma)$ denotes the set of conjugacy classes of elliptic elements in Γ,
- for an elliptic element $\gamma\in\Gamma$, $m(\gamma)$ denotes its order and $\theta(\gamma)$ denotes half the angle of rotation, i.e., is such that γ is conjugate to
$$\begin{bmatrix} \cos(\theta(\gamma)) & \sin(\theta(\gamma)) \\ -\sin(\theta(\gamma)) & \cos(\theta(\gamma)) \end{bmatrix} \in \mathrm{PSL}(2,\mathbb{R}),$$
- $\mathcal{P}(\Gamma)$ denotes the set of conjugacy classes of primitive hyperbolic elements in Γ,
- for a hyperbolic element $\gamma\in\Gamma$, $\ell(\gamma)$ denotes its translation length on $\mathbb{H}^2$.

Moreover, on the left-hand side (the spectral side) we may use any of the two branches of the square root, because $\widehat{f}$ is even.

We will write $\mathcal{G}(\Gamma,\phi,f)$ for the right-hand side (the geometric side) of the twisted Selberg trace formula (2.1) in the case that φ is induced by $\phi: G\to\mathrm{GL}(V)$.

2.4. **Simplifications in the trace formula.** It is possible to express the geometric side of the trace formula entirely in terms of the function f (instead of its Fourier transform $\widehat{f}$). In our application, f will be compactly supported, so writing the geometric side in terms of it will make the integrals that appear easier to estimate rigorously.

The identity and elliptic terms on the geometric side of (2.1) can be written as:

$$\int_{-\infty}^{\infty} y\widehat{f}(y)\tanh(\pi y)dy = -\int_{-\infty}^{\infty}\frac{f'(x)}{\sinh(x/2)}dx$$

and

$$\frac{1}{2\sin(\theta)}\int_{-\infty}^{\infty}\frac{e^{-2\theta\cdot y}}{1+e^{-2\pi y}}\widehat{f}(y)dy = \int_0^{\infty}\frac{\cosh(x/2)}{\cosh(x)-1+2\sin(\theta)^2}f(x)dx,$$

see [Hej76, p. 27-28, 450].

3. Excluding representations

In this section, we explain how to prove lower bounds on the eigenvalues of the Laplacian twisted by an irreducible representation ϕ. In view of Proposition 2.1, this implies that ϕ cannot appear in an eigenspace of Δ on $\Lambda\backslash\mathbb{H}^2$ for eigenvalues below such a bound. We will apply this criterion in Section 5 to exclude all but the top-dimensional irreducible

representations from appearing in the eigenspaces corresponding to $\lambda_1(X_{10})$ and $\lambda_1(X_{17})$, where X_{10} and X_{17} are the surfaces from Theorem 1.1.

3.1. **The criterion.** Our main tool for excluding representations is derived from the twisted Selberg trace formula. A similar criterion is behind the method of Booker–Strömbergsson [BS07] to which we will come back below. We still assume that $\Lambda < \Gamma$ are co-compact Fuchsian groups and $G = \Gamma/\Lambda$ is finite as in Section 2.

Proposition 3.1. *Let $\phi \in \mathrm{Irr}(G)$, let $\lambda > 0$, and suppose that there exists an admissible function $f : \mathbb{R} \to \mathbb{R}$ such that $\widehat{f}\left(\sqrt{\mu - \frac{1}{4}}\right) \geq 0$ for all $\mu \geq 0$ and*

$$\widehat{f}\left(\sqrt{\lambda - \frac{1}{4}}\right) > \begin{cases} \mathcal{G}(\Gamma, \phi, f) & \text{if } \phi \text{ is non-trivial} \\ \mathcal{G}(\Gamma, \phi, f) - \widehat{f}(i/2) & \text{if } \phi \text{ is trivial.} \end{cases}$$

Then $\lambda \notin \mathrm{spec}(\Gamma\backslash\mathbb{H}^2, \phi)$.

Proof. Suppose for a contradiction that $\lambda \in \mathrm{spec}(\Gamma\backslash\mathbb{H}^2, \phi)$. By the twisted Selberg trace formula (2.1) and the non-negativity hypothesis on $\widehat{f}$, we have

$$\widehat{f}\left(\sqrt{\lambda - \frac{1}{4}}\right) \leq \sum_{\mu \in \mathrm{spec}(\Gamma\backslash\mathbb{H}^2, \phi)} \widehat{f}\left(\sqrt{\mu - \frac{1}{4}}\right) = \mathcal{G}(\Gamma, \phi, f),$$

which is a contradiction if ϕ is non-trivial. If ϕ is trivial, then $0 \in \mathrm{spec}(\Gamma\backslash\mathbb{H}^2, \phi)$ so that we have

$$\widehat{f}(i/2) + \widehat{f}\left(\sqrt{\lambda - \frac{1}{4}}\right) \leq \sum_{\mu \in \mathrm{spec}(\Gamma\backslash\mathbb{H}^2, \phi)} \widehat{f}\left(\sqrt{\mu - \frac{1}{4}}\right) = \mathcal{G}(\Gamma, \phi, f),$$

which is again a contradiction. □

In practice, we will use the same function f for all λ in some interval $(0, b]$, which will prove that $\mathrm{spec}(\Gamma\backslash\mathbb{H}^2, \phi) \cap (0, b] = \varnothing$.

3.2. **Test functions.** Given $d > 0$, we define the following admissible pair

$$f_d(x) = \left(\frac{1}{2d}\chi_{[-d,d]}\right)^{*4}(x) \quad \text{and} \quad \widehat{f_d}(y) = \frac{\sin(d \cdot y)^4}{(d \cdot y)^4},$$

where $\chi_{[-d,d]}$ denotes the characteristic function of the interval $[-d, d]$ and the exponent $*4$ denotes the fourfold convolution product of the function with itself. An elementary computation yields that

$$f_d(x) = \begin{cases} \frac{1}{12d}\left(4 - \frac{3}{2d^2}x^2 + \frac{3}{8d^3}|x|^3\right) & \text{if } 0 \leq |x| \leq 2d, \\ \frac{1}{12d}\left(2 - \frac{|x|}{2d}\right)^3 & \text{if } 2d \leq |x| \leq 4d \text{ and} \\ 0 & \text{otherwise.} \end{cases}$$

In particular,

$$\mathrm{supp}(f_d) = [-4d, 4d].$$

The method of Booker–Strömbergsson [BS07] is based on functions that are linear combinations of shifts of test functions of this type. This method is very effective for estimating the spectrum of hyperbolic orbifolds and has been applied in various other contexts since [LL22a, LL22b, LL21, BMP23, GPSDX23]. We initially applied this method here as well, but then realized that just one test function was enough for our purposes.

Observe that $\widehat{f_d}$ is non-negative on the real and imaginary axes. Furthermore, it is increasing along the positive imaginary axis and decreasing on the interval $[0, \pi/d]$, so that $\widehat{f_d}\left(\sqrt{\lambda - 1/4}\right)$ is decreasing for $\lambda \in [0, (\pi/d)^2 + 1/4]$. It follows that if the inequality in Proposition 3.1 is satisfied at $\lambda = b \leq (\pi/d)^2 + 1/4$, then it is also satisfied for every $\lambda \in (0, b]$.

The fact that f_d has compact support is useful for us, because it means that if we know all the elliptic conjugacy classes and all the conjugacy classes of primitive hyperbolic elements of translation length at most $4d$ in our Fuchsian group Γ, then we can compute the geometric side $\mathcal{G}(\Gamma, \phi, f_d)$ in the twisted Selberg trace formula. Since X_{10} and X_{17} are triangle surfaces, the corresponding Fuchsian groups (that will play the role of Λ) are normal subgroups of triangle groups (that will play the role of Γ). In that case, the conjugacy classes of elliptic elements are simply the conjugacy classes of the standard generators x, y, z (see Section 4.3) and their powers. In the next section, we will explain how to list the primitive hyperbolic conjugacy classes of small translation length in these groups.

4. Generating conjugacy classes

Given a cocompact Fuchsian group $\Gamma < \mathrm{PSL}(2, \mathbb{R})$ and a real number $L > 0$, we need an algorithm that lists the distinct conjugacy classes of primitive hyperbolic elements in Γ with translation length at most L. Such an algorithm is described in [HW94] for hyperbolic 3-orbifolds and is used in the computer program `SnapPy`. The same algorithm works in dimension 2 as well. We describe this algorithm with minor modifications below.

The idea is to generate enough elements in Γ to cover a ball of a certain radius $R = R(L)$ around a basepoint $x_0 \in \mathbb{H}^2$ by images of a fundamental domain. We then check for conjugacy between all pairs of hyperbolic elements with translation length at most L via the elements in the previous list. Finally, we delete the conjugacy classes of non-primitive elements by checking if they are (conjugate to) powers of other elements. Throughout, we use interval arithmetic to make numerical calculations rigorous.

4.1. The word problem.

To test for conjugacy, we first need to be able to test whether two elements $f, g \in \Gamma$ are equal. In theory, this should be easy: for any fixed pair of distinct points $x_0, x_1 \in \mathbb{H}^2$, we have that $f = g$ if and only if they agree on x_0 and x_1.

The problem comes when we try to do this on the computer, where arbitrary real numbers cannot be represented exactly. Instead, we represent elements of Γ as 2 by 2 matrices whose entries lie in certain intervals with exact endpoints. All calculations performed subsequently keep track of correct intervals containing the answers by rounding upper and lower bounds appropriately. This is called *interval arithmetic*.

The drawback is that we only know elements of Γ up to a certain precision, but the redeeming feature is that Γ is discrete, so we can still tell elements apart if the precision is good enough. To be precise, fix two distinct points x_0 and x_1 and let δ_j be the smallest distance between two distinct points in the Γ-orbit of x_j. If $f, g \in \Gamma$, we want to determine if $f(x_0) = g(x_0)$ and $f(x_1) = g(x_1)$, which is equivalent to

$$d(f(x_0), g(x_0)) < \delta_0 \quad \text{and} \quad d(f(x_1), g(x_1)) < \delta_1.$$

On the other hand, if either distance is strictly positive, then $f \neq g$. In theory, if there is too much imprecision on $f(x_j)$ or $g(x_j)$, then the computer might not be able to decide if the above inequalities hold or not, but we have not encountered that possibility in practice.

We will apply the above criterion when Γ is a triangle group, where we take x_0 and x_1 to be fixed points of elliptic elements and δ_0 and δ_1 can be computed explicitly.

4.2. **The conjugacy problem.** Let $F \subset \mathbb{H}^2$ be a compact fundamental domain for Γ. If $\gamma \in \Gamma$ is hyperbolic, we denote its translation axis (the geodesic between its two fixed points at infinity) by $\operatorname{axis}(\gamma)$. If $h \in \Gamma$, then observe that $\operatorname{axis}(h\gamma h^{-1}) = h(\operatorname{axis}(\gamma))$. Since for every $y \in \mathbb{H}^2$ there is some $h \in \Gamma$ such that $h(y) \in F$, any hyperbolic element $\gamma \in \Gamma$ has a conjugate $h\gamma h^{-1}$ whose axis intersects F. If D is the diameter of F and $x_0 \in F$ is some basepoint, then in particular the axis of $h\gamma h^{-1}$ is within distance D of x_0. In [HW94], Hodgson and Weeks make this more efficient by using the largest distance from x_0 to an edge of F instead of the diameter, assuming that F is a Dirichlet fundamental domain.

Although there are more hyperbolic elements whose axis passes within distance D of x_0 than whose axis intersects F, the former condition is easier to test.

Lemma 4.1. *Let $\gamma \in \mathrm{PSL}(2, \mathbb{R})$ be a hyperbolic element with translation length ℓ, let $x_0 \in \mathbb{H}^2$, and let δ be the distance between x_0 and $\operatorname{axis}(\gamma)$. Then*

$$\sinh(d(x_0, \gamma(x_0))/2) = \sinh(\ell/2)\cosh(\delta).$$

Proof. Form a Saccheri quadrilateral with x_0, $\gamma(x_0)$ and their orthogonal projections onto $\operatorname{axis}(\gamma)$, then divide it into two congruent Lambert quadrilaterals along its axis of symmetry. The resulting Lambert quadrilateral has a short side of length $\ell/2$, the opposite side of length $d(x_0, \gamma(x_0))/2$, and the longer of the two remaining sides of length δ. The equation stated is Formula 2.3.1(v) in [Bus10, p.454] applied to this quadrilateral. □

This means that we do not have to compute the translation axes of hyperbolic elements, nor do we need to check if they intersect the sides of the fundamental domain F. These operations would be cumbersome on the computer given that the elements of Γ are not represented exactly.

By Lemma 4.1, to generate all hyperbolic elements in Γ of translation length at most L whose axes pass within distance D from x_0 it suffices to generate all the elements that move x_0 by distance at most

$$r = 2\operatorname{arcsinh}(\sinh(L/2)\cosh(D)).$$

In other words, it suffices to generate a set $E \subset \Gamma$ such that $\bigcup_{\gamma \in E} \gamma(F)$ contains the closed ball of radius r around x_0, which is something we can test by computing the minimum

distance from x_0 to any side of $\bigcup_{\gamma\in E}\gamma(F)$. Note that our formula for r is smaller than the one used in [HW94] because we are working in dimension 2. In dimension 3, a hyperbolic element can act as a screw motion along an axis, which increases the distance between x_0 and $\gamma(x_0)$.

The next thing we need is a stopping criterion to test for conjugacy between hyperbolic elements in the set E.

Lemma 4.2. *Suppose that $\alpha, \beta \in \Gamma$ are conjugate hyperbolic elements of translation length ℓ whose axes intersect the closed ball of radius D around $x_0 \in \mathbb{H}^2$. Then there is some $h \in \Gamma$ such that $\beta = h\alpha h^{-1}$ and*

$$d(x_0, h(x_0)) \leq 2\operatorname{arccosh}(\cosh(\ell/4)\cosh(D)).$$

Proof. Let $h_0 \in \Gamma$ be an element that conjugates α and β. Then $h_0(\operatorname{axis}(\alpha)) = \operatorname{axis}(\beta)$. In particular,

$$d(h_0(x_0), \operatorname{axis}(\beta)) = d(x_0, \alpha) \leq D.$$

Let z be the point on $\operatorname{axis}(\beta)$ closest to x_0 and let w_0 be the orthogonal projection of $h_0(x_0)$ onto that axis. Observe that we can replace h_0 with $h = \beta^k h_0$ for any $k \in \mathbb{Z}$ and still have $\beta = h\alpha h^{-1}$. Choose k in such a way that $w = \beta^k(w_0)$ satisfies $d(z, w) \leq \ell/2$. If m is the midpoint between z and w, then

$$d(x_0, h(x_0)) \leq d(x_0, m) + d(m, h(x_0)).$$

Each of the last two distances is the hypothenuse of a right triangle with legs of length at most $\ell/4$ and D. The stated inequality then follows from the hyperbolic Pythagorean theorem [Bus10, Equation 2.2.2(i), p.454]. □

The conclusion is that it suffices to generate enough elements to cover the ball of radius

$$R = \max\left\{2\operatorname{arcsinh}(\sinh(L/2)\cosh(D)), 2\operatorname{arccosh}(\cosh(L/4)\cosh(D))\right\}$$

around x_0 by translates of F in order to solve our problem. We explain how to do this efficiently in the special case where Γ is a $(2, 3, r)$-triangle group with $r \geq 7$ in the next subsection.

4.3. **An explicit automatic structure for some triangle groups.** For integers $p, q, r \geq 2$ with $\frac{1}{p} + \frac{1}{q} + \frac{1}{r} < 1$, the *$(p, q, r)$-triangle group* $T(p, q, r)$ (unique up to conjugation in $\mathrm{PSL}(2, \mathbb{R})$) is the group generated by rotations x, y, z of counterclockwise angles $\frac{2\pi}{p}$, $\frac{2\pi}{q}$, and $\frac{2\pi}{r}$ around the vertices of a triangle τ_0 in $\mathbb{H}^2$ with interior angles $\frac{\pi}{p}$, $\frac{\pi}{q}$, and $\frac{\pi}{r}$ appearing in this order counterclockwise around τ_0. This group is discrete and cocompact, and admits the presentation

$$T(p, q, r) \cong \langle x, y, z : x^p = y^q = z^r = xyz = \mathrm{id}\rangle.$$

To generate elements of a group efficiently, it is useful to do it without redundancy, especially when the group has exponential growth. This is precisely what automatic structures are for. Note that every cocompact Fuchsian group is word-hyperbolic and every word-hyperbolic group is automatic (see e.g. [ECH+92, Section 3.4]). There also exist algorithms to compute finite state automata for such groups (see [ECH+92, Chapter 5]

and [EH00]). However, it is more convenient if automata are readily available. For triangle groups $T(p,q,r)$ with $p,q,r \geq 6$, explicit automatic structures were found in [Pfe08]. This does not cover the cases $T(2,3,7)$ and $T(2,3,8)$ that we need. An automaton for $T(2,3,7)$ was described without proof in [CKK22, Example 1] and is used in the video game `HyperRogue`. We generalize this automaton to groups $T(2,3,r)$ with $r \geq 7$ and provide a proof below. The automaton also works for the triangle group $T(2,3,6)$ acting on the euclidean plane.

Let A, B, and C be the centers of rotation of x, y, and z respectively (the vertices of τ_0) and let F be the union of τ_0 with its reflection about the geodesic through A and C. This is a fundamental domain for the action of $T(p,q,r)$ in general. It is also true that F is a Dirichlet fundamental domain for any point in the interior of the segment between A and C. However, it seems more natural to use $x_0 = C$ as basepoint when applying the results of subsection 4.2 due to the symmetries of the tiling of $\mathbb{H}^2$ by (p,q,r)-triangles.

If $p = 2$ (in which case F is an isoceles triangle) and $q = 3$, then $P_0 = \bigcup_{k=0}^{r-1} z^k(F)$ is a regular r-gon with interior angles $2\pi/3$. The distinct images of P_0 by $T_r = T(2,3,r)$ form a tiling $\mathcal{P}$ of $\mathbb{R}^2$ or $\mathbb{H}^2$ and the elements of T_r are in bijection with the oriented edges in this tiling. Concretely, the identity element is associated to the edge e_0 of F opposite to the vertex C and oriented so that F is to its left, and then any element $g \in T_r$ is associated to the edge $g(e_0)$.

Observe that it is more natural for T_r (or any group) to act on the right on oriented edges (or images of any fixed object). That is, suppose that g acts on e_0 in a certain way, say by rotating it by π around its midpoint (as x does) or moving it to the next edge forward and to the left in the tiling (as z does). Then to perform the same movement from an oriented edge $f(e_0)$ in the tiling, we must apply the conjugate transformation fgf^{-1} on the left, which yields the edge $fg(e_0)$. One way to say this is that a group acts on images of a given object by *instructions* on the right. Therefore, if an element $w \in T_r$ is written as a word in the generators x and z, then the edge $w(e_0)$ is obtained by starting with e_0 and then applying the instructions given by the letters in w, read from left to right.

To generate T_r, the basic idea is to start with the polygon P_0 and move to the adjacent polygons using the rotations of angle π around the midpoints of its edges to obtain the adjacent polygons. Once we enter a new polygon, we go around its edges by rotating around its center. At each step, we want to cover all the polygons adjacent to the previous polygons, but only once.

The finite state automaton we use for T_r has four states L(eft), M(iddle), R(ight), I(n) in addition to the initial state $\varnothing$. The possible transitions between different states are given in Figure 2. For the purpose of generating the group, one could merge the states I and R into a single one, but it is useful to keep them separate in order to compute the boundary of the region of the tiling covered after some number of iterations.

Let us describe what the automaton does in words instead of using the formal terminology from the theory of automata. We start with the set $E_1 := \{\mathrm{id}, z, \ldots, z^{r-1}\}$ whose elements are all assigned the label M except for the identity which has the label $\varnothing$. Then for each $n \geq 1$, the next generation E_{n+1} is defined as the union of the children of all the elements $g \in E_n$, with the following rules:

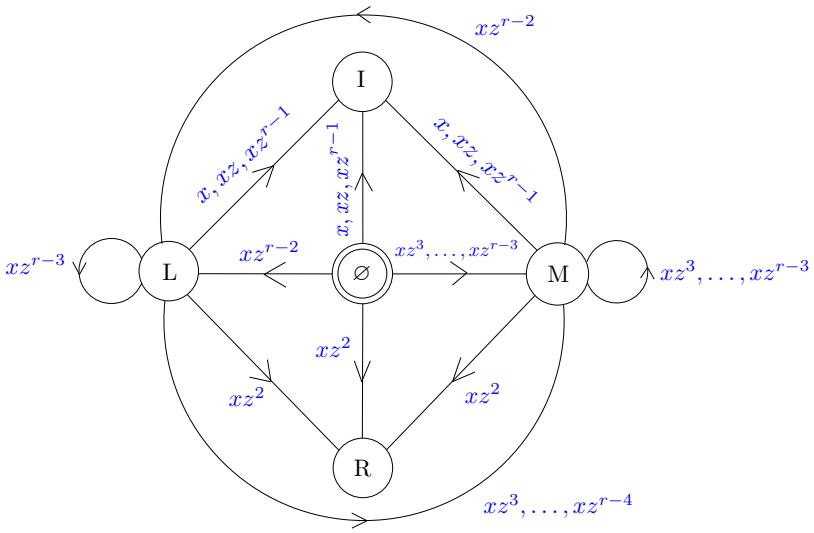

FIGURE 2. A picture of the automaton generating the elements of $T(2,3,r)$. We have drawn the partial automaton (i.e., without dead states). The initial state (center) and the states L, M, R, I are all accepted. Multiplication is on the right and the empty word represents the identity.

(1) if g has label I or R, then g has no children;

(2) otherwise, the children of g are gxz^j for $0 \leq j \leq r-1$, with the following labels:

   (a) gxz^{r-1}, gx, and gxz have label I;

   (b) gxz^2 has label R;

   (c) if g has label M or $\varnothing$, then gxz^j has label M if $3 \leq j \leq r-3$ and L if $j = r-2$;

   (d) if g is L, then gxz^j has label M if $3 \leq j \leq r-4$, L if $j = r-3$, and I if $j = r-2$.

We now prove that this is indeed an automaton for the group T_r.

Proposition 4.3. *For every $r \geq 6$, the above automaton eventually generates every element of the triangle group $T(2,3,r)$ and it does so exactly once.*

Proof. Since the map from $T_r = T(2,3,r)$ to polygons in the tiling $\mathcal{P}$ sending $g \in T_r$ to $g(P_0)$ is r-to-1 and since every element g with descendents has r children gxz^j for $0 \leq j \leq r-1$ all yielding the same polygon, it suffices to check that every polygon in $\mathcal{P}$ except P_0 is obtained exactly once as the first-born child $gx(P_0)$ of an element g. Note that $g(P_0)$ and $gx(P_0)$ are adjacent along the side $g(e_0)$.

For every $n \geq 1$, let $\mathcal{L}_n = \bigcup_{g \in E_n} g(P_0)$ be the union of the polygons produced at generation n. We will prove by induction that

(1) $\mathcal{L}_n$ is the union of polygons adjacent to the outer boundary of $\mathcal{L}_{n-1}$;

(2) the outer boundary of $\mathcal{L}_n$ consists of the edges of generation n that are labelled L, M, or R;

(3) $\mathcal{L}_n$ forms a cycle of polygons, meaning that each polygon in $\mathcal{L}_n$ is adjacent to (shares a side with) exactly two others in $\mathcal{L}_n$;

(4) each polygon in $\mathcal{L}_n$ is the first-born child $gx(P_0)$ of a unique element g in E_{n-1};

for every $n \geq 2$.

The statements are obvious for $n = 2$, where $\mathcal{L}_2$ is formed of the r polygons adjacent to $\mathcal{L}_1 = P_0$. For every $g \in E_1$, the side $gx(e_0)$ of $gx(P_0)$ is on the inner boundary of $\mathcal{L}_2$ while the sides $gxz^{\pm 1}(e_0)$ are shared with the two neighboring polygons $gz^{\pm 1}x(P_0)$. The remaining sides of $\mathcal{L}_2$ form a cycle whose labels form the string $(\mathrm{LM}^{r-5}\mathrm{R})^r$, when read clockwise (see Figure 3 for an example). Furthermore, the r polygons $gx(P_0)$ for $g \in E_1$ are distinct.

Suppose the above statements are true for $n = k \geq 2$ and let us prove them for $n = k+1$. We will prove them in order.

Proof of (1): By item (2), then only active elements in E_k (those with label L or M) are on the outer boundary. This implies that $\mathcal{L}_{k+1}$ is contained in the union of polygons adjacent to the outer boundary of $\mathcal{L}_k$. It remains to show that the polygons adjacent to the edges labelled R are also contained in $\mathcal{L}_{k+1}$. This is true because the edge $g(e_0)$ following an edge s with label R in $\partial\mathcal{L}_k$ in clockwise order is the first exposed edge of the following polygon in the cycle, hence is labelled L. Therefore, the polygon $gx(P_0)$ is produced at generation $k+1$, and this polygon is adjacent to both $g(e_0)$ and s since there are only three polygons around each vertex in $\mathcal{P}$. This proves that (1) holds for $n = k + 1$.

Proof of (2): Again using item (2), the labels along the outer boundary of $\mathcal{L}_k$ form a cycle of strings of the form $\mathrm{LM}^{r-5}\mathrm{R}$ or $\mathrm{LM}^{r-6}\mathrm{R}$ (see Figure 3 for an example). Observe that each such string corresponds to the (consecutive) outer edges of a single polygon P in $\mathcal{L}_k$. The polygons adjacent to P across the L and M sides therefore form a sequence, each adjacent to the next. Furthermore, the polygon Q adjacent to P through the L side contains the R edge of the preceeding string s, so that it is adjacent to the last polygon in the corresponding sequence of polygons. This means that the sequences of polygons link up nicely, and they form a closed cycle because the outer boundary of $\mathcal{L}_k$ closes up.

For each of these strings $\mathrm{LM}^m\mathrm{R}$, and for each edge $g(e_0)$ with label M in that string, the edge $gx(e_0)$ is on the inner boundary of $\mathcal{L}_{k+1}$ while $gxz^{\pm 1}(e_0)$ are shared between consecutive polygons in $\mathcal{L}_{k+1}$, hence are in the interior. For the edge $g(e_0)$ with label L, $gx(e_0)$ and $gxz^{-1}(e_0)$ are both on the inner boundary ($gxz^{-1}(e_0)$ coincides with the edge labelled R in the preceeding string), while $gxz(e_0)$ and $gxz^{-2}(e_0)$ are in the interior. This is why all these edges are labelled I according to our rules. As such, (2) holds for $n = k+1$.

Proof of (3): Now, consider the edges labelled L, M, or R in $\mathcal{L}_{k+1}$. By the last two paragraphs, these form a closed loop α in the hyperbolic plane, following the outer boundary of a cycle of polygons. However, this cycle of polygons could in principle be not embedded, meaning that two polygons far apart in the cycle could be adjacent or even coincide. To prove that it is embedded, observe that the interior angles of α are $2\pi/3$ except at junctions

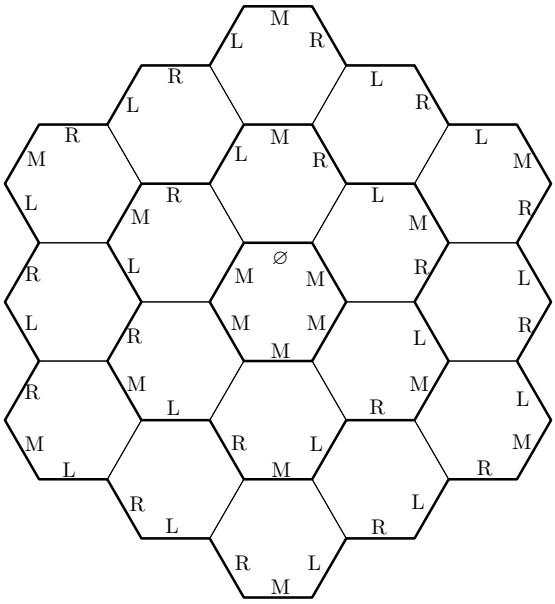

FIGURE 3. The labels assigned to edges on the outer boundary of some layers in the tiling associated with the triangle group $T(2,3,6)$. The remaining edges are all labelled I.

between R and L edges, where the interior angle is $4\pi/3$. Replace each such inward corner by the geodesic between its endpoints. This increases the interior angle at the adjacent vertices, but by not more than $\frac{\pi}{6}+\frac{\pi}{6}$, for a total of at most $\frac{2\pi}{3}+\frac{\pi}{6}+\frac{\pi}{6}=\pi$. The resulting curve is therefore convex, hence embedded, and therefore so is α. It follows that the cycle of polygons in $\mathcal{L}_{k+1}$ is also embedded, completing the proof of (3) for $n=k+1$.

Proof of (4): By construction, our cycle of polygons was obtained as the set of first-born children of the L and M elements in E_k. We have just shown that these are all distinct, which is statement (4) for $n=k+1$ and completes the induction step.

Now consider the set $U=\bigcup_{n=1}^{\infty}\mathcal{L}_n$. This set is open since $\bigcup_{n=1}^{m}\mathcal{L}_n$ is in the interior of $\bigcup_{n=1}^{m+1}\mathcal{L}_n$ by item (1) above. It is also complete. Indeed, suppose that $(z_k)_{k=1}^{\infty}$ is a Cauchy sequence in U. By shifting the sequence we may assume that its diameter is at most the length of any edge in the tiling $\mathcal{P}$. Thus, if $z_1\in\bigcup_{n=1}^{m}\mathcal{L}_n$ then the entire sequence is contained in $\bigcup_{n=1}^{m+1}\mathcal{L}_n$, which is compact, hence complete. We conclude that the sequence $(z_k)_{k=1}^{\infty}$ converges in U, so that U is complete. In particular, U is closed. Since $\mathbb{R}^2$ and $\mathbb{H}^2$ are connected and U is non-empty, U is equal to the whole space.

We conclude that every polygon P in $\mathcal{P}\setminus P_0$ is contained in some $\mathcal{L}_n$. Since the layers $\mathcal{L}_j$ all have disjoint interiors, n is unique and the parents of P are necessarily contained in E_{n-1} by (1). Lastly, the parent is unique by (4). □

We use this automaton to generate elements in the group $T(2,3,r)$ until we cover a large enough ball around the point $x_0=C$ to capture all conjugacy classes of hyperbolic elements of translation length at most L (and test for conjugacy between them). In order

to compute the inner radius of the region covered after n generations, we use the fact that its boundary is the set of edges in the last generation with labels different from I. We then measure the distance from C to each of these edges and take the minimum. Since the distance function is convex, the distance from C to an edge e is either the height of the triangle with base e and opposite vertex C, or the minimum of the lengths of the two other edges, depending on whether the altitude is contained in the triangle or not.

The resulting algorithm is implemented in the `Jupyter` notebook `generate_classes` (to be used with `SageMath`) attached as an ancillary file with the arXiv version of this paper. The program outputs lists of primitive conjugacy classes up to any desired translation length for any $r \geq 7$. These lists of conjugacy classes are then fed as input in two other programs to compute the geometric side of the twisted Selberg trace formula for the irreducible representations of the orientation-preserving isometry groups of the surfaces X_{10} and X_{17}.

5. Finishing the proof

In this last section, we combine the ingredients of the previous sections to prove Theorem 1.1. We first describe the surfaces X_{10} and X_{17} and recall the strategy of proof. We then explain which part the computer does for us and how these calculations imply the result.

5.1. **The surfaces.** We have not fully described the surfaces X_{10} and X_{17} from Theorem 1.1 yet. They are defined as $X_g = \Lambda_g \backslash \mathbb{H}^2$ for some torsion-free finite-index normal subgroups $\Lambda_{10} < T(2,3,8)$ and $\Lambda_{17} < T(2,3,7)$. In turn, these groups are defined as the normal closures

$$\Lambda_{10} = \langle\langle\ (zyxz)^2 yz^{-1}xy^{-1}z^{-2}xz\ \rangle\rangle^{T(2,3,8)}$$

and

$$\begin{aligned}\Lambda_{17} = \langle\langle\ & z^{-3}xyz^{-3},\\ & xzyxzyxy^{-1}z^{-1}xy^{-1}z^{-1}xy^{-1}z^{-1}xy^{-1}z^{-1}xy^{-1}z^{-1}xy^{-1}z^{-1},\\ & zyxzyz^{-1}xzy^{-1}z^{-1}xy^{-1}z^{-2}xzy^{-1}z^{-1}xy^{-1}z^{-2}xz\ \rangle\rangle^{T(2,3,7)}\end{aligned}$$

where x, y, and z are the standard generators of order p, q, and r in $T(p,q,r)$. We also write $G_{10} := T(2,3,8)/\Lambda_{10}$ and $G_{17} := T(2,3,7)/\Lambda_{17}$.

These groups were taken from the list [Con15] of all triangle surfaces of genus at most 101 calculated by Conder using algorithms explained in [Con84]. The groups G_{10} and G_{17} appear as `T10.1` and `T17.1` in Conder's list.

For completeness, we verify that X_{10} and X_{17} are indeed surfaces without cone points and of the correct genera 10 and 17 in the `Jupyter` notebooks `verify_genus_10` and `verify_genus_17` attached as ancillary files with the arXiv version of this paper. We also use `SageMath` and `GAP` to compute the character tables of G_{10} and G_{17}; the results can be found in Appendix A.

5.2. **Set-up and strategy.** First, we fix the parameters that will appear in the proof.

- We set $\lambda_1^{\max}(10) = 1.223$ and $\lambda_1^{\max}(17) = 0.969$.
- We set $\Gamma_{10} = T(2,3,8)$ and $\Gamma_{17} = T(2,3,7)$.
- $\mu_{10} = 16$ and $\mu_{17} = 21$ are the multiplicities we want to prove (the maximal dimensions of irreps of G_{10} and G_{17}).
- The parameter d we choose equals $L/4$ (so that f_d has support $[-L, L]$), where $L = 3$ is the translation length up to which we list the primitive hyperbolic conjugacy classes in Γ_{10} and Γ_{17}.

Note that $\lambda_1^{\max}(17) < \lambda_1^{\max}(10) < 17.795 \approx \left(\frac{\pi}{d}\right)^2 + \frac{1}{4}$ so that $\widehat{f_d}\left(\sqrt{\lambda - \frac{1}{4}}\right)$ is decreasing on the interval $(0, \lambda_1^{\max}(g)]$ for $g \in \{10, 17\}$. Our goal is then to prove that $\widehat{f_d}\left(\sqrt{\lambda_1^{\max}(g) - \frac{1}{4}}\right)$ is strictly larger that the right-hand side in Proposition 3.1 for all irreducible representations ϕ of G_g of real dimension less than μ_g. This requires estimating the different terms on the geometric side of the twisted Selberg trace formula with sufficient precision.

5.3. **Formal verification.** We have performed the formal verification of the inequalities we are after using `SageMath`. The full code is available in the ancillary files `verify_genus_10` and `verify_genus_17`. We outline the steps here:

(1) We use the interface to `GAP` in order to determine all the irreducible representations of the groups G_g for $g \in \{10, 17\}$. We have decided to work over $\mathbb{R}$, so we convert the characters `GAP` gives us to real characters (using [Ser77, Proposition 39]).

(2) We use interval arithmetic and our lists of primitive hyperbolic conjugacy classes generated by the file `generate_classes` to estimate the last sum in $\mathcal{G}(\Gamma_g, \phi, f_d)$.

(3) For the elliptic and identity terms, we use the formulas in terms of f_d from Section 2.4; this avoids having to estimate indefinite integrals. The integrals that do appear are treated using interval arithmetic as implemented in the `Arb` package. The integral for the identity term is slightly trickier because the integrand is a quotient of two functions that vanish at the origin. We use a Taylor approximation with error estimate near zero to get around this issue.

5.4. **The proof.** In this final subsection, we gather our results.

Proof of Theorem 1.1. By the results of our computer code (`verifiy_genus_10` and `verifiy_genus_17`),

$$\widehat{f_d}\left(\sqrt{\lambda - \frac{1}{4}}\right) \quad > \quad \begin{cases} \mathcal{G}(\Gamma_g, \phi, f_d) & \text{for all non-trivial } \phi \in \mathrm{Irr}(G_g) \\ & \text{with } \dim_{\mathbb{R}}(\phi) < \mu_g \\ \mathcal{G}(\Gamma_g, \phi, f_d) - \widehat{f_d}(i/2) & \text{for the trivial representation } \phi \in \mathrm{Irr}(G_g) \end{cases}$$

at $\lambda = \lambda_1^{\max}(g)$ and therefore for all $\lambda \in (0, \lambda_1^{\max}(g)]$ as well, for both $g = 10$ and $g = 17$.

By Proposition 3.1, this means that $\mathrm{spec}(\Gamma_g \backslash \mathbb{H}^2, \phi)$ is disjoint from $(0, \lambda_1^{\max}(g)]$ for every $\phi \in \mathrm{Irr}(G_g)$ with $\dim_{\mathbb{R}}(\phi) < \mu_g$. Therefore, every eigenvalue in $\mathrm{spec}(\Lambda_g \backslash \mathbb{H}^2) \cap (0, \lambda_1^{\max}(g)]$ has multiplicity equal to a sum of dimensions $\dim_{\mathbb{R}}(\phi)$ for representations $\phi \in \mathrm{Irr}(G_g)$

of real dimension at least (hence equal to) μ_g by Proposition 2.1. We also know that $\lambda_1(X_g) \in (0, \lambda_1^{\max}(g)]$ by [FBP23b, Table 3], so that $m_1(X_{10}) = 16k_{10}$ and $m_1(X_{17}) = 21k_{17}$ for some integers $k_{10}, k_{17} \geq 1$. From [FBP23b, Table 5], we know that $m_1(X_{10}) \leq 20$ and $m_1(X_{17}) \leq 34$ (Sévennec's bound $2g+3$ [Sév02] would also work), from which we conclude that $k_{10} = k_{17} = 1$, hence $m_1(X_{10}) = 16$ and $m_1(X_{17}) = 21$ as required. □

Remark 5.1. For G_{17}, our computer program is able to exclude the irreducible representation corresponding to χ_{11} in Table 2, so it is the irreducible representation corresponding to χ_{10} that appears in the first eigenspace.

References

[AH77] K. Appel and W. Haken, *Every planar map is four colorable. I. Discharging*, Illinois J. Math. **21** (1977), no. 3, 429–490.

[AHK77] K. Appel, W. Haken, and J. Koch, *Every planar map is four colorable. II. Reducibility*, Illinois J. Math. **21** (1977), no. 3, 491–567.

[BC85] M. Burger and B. Colbois, *À propos de la multiplicité de la première valeur propre du laplacien d'une surface de Riemann*, C. R. Acad. Sci. Paris Sér. I Math. **300** (1985), no. 8, 247–249.

[Bes80] G. Besson, *Sur la multiplicité de la première valeur propre des surfaces riemanniennes*, Ann. Inst. Fourier (Grenoble) **30** (1980), no. 1, x, 109–128.

[Bes87] ———, *Sur la multiplicité des valeurs propres du laplacien*, Séminaire de Théorie Spectrale et Géométrie, No. 5, Année 1986–1987, Univ. Grenoble I, Saint-Martin-d'Hères, 1987, pp. 107–132.

[BMP23] J. Bonifacio, D. Mazac, and S. Pal, *Spectral bounds on hyperbolic 3-manifolds: Associativity and the trace formula*, preprint, arXiv:2308.11174, 2023.

[BS07] A. R. Booker and A. Strömbergsson, *Numerical computations with the trace formula and the Selberg eigenvalue conjecture*, J. Reine Angew. Math. **607** (2007), 113–161. MR 2338122

[Bus10] P. Buser, *Geometry and spectra of compact Riemann surfaces*, Modern Birkhäuser Classics, Birkhäuser Boston, Inc., Boston, MA, 2010, Reprint of the 1992 edition.

[CCdV88] B. Colbois and Y. Colin de Verdière, *Sur la multiplicité de la première valeur propre d'une surface de Riemann à courbure constante*, Comment. Math. Helv. **63** (1988), no. 2, 194–208. MR 948777

[CdV86] Y. Colin de Verdière, *Sur la multiplicité de la première valeur propre non nulle du laplacien*, Comment. Math. Helv. **61** (1986), no. 2, 254–270.

[CdV87] ———, *Construction de laplaciens dont une partie finie du spectre est donnée*, Ann. Sci. École Norm. Sup. (4) **20** (1987), 599–615.

[Che76] S. Y. Cheng, *Eigenfunctions and nodal sets*, Comment. Math. Helv. **51** (1976), no. 1, 43–55.

[CKK22] D. Celińska-Kopczyńska and E. Kopczyński, *Generating tree structures for hyperbolic tessellations*, preprint, arXiv:2111.12040, 2022.

[Con84] M. D. E. Conder, *Some results on quotients of triangle groups*, Bull. Austral. Math. Soc. **30** (1984), no. 1, 73–90.

[Con15] ———, *Quotients of triangle groups acting on surfaces of genus 2 to 101*, math.auckland.ac.nz/∼conder/TriangleGroupQuotients101.txt, 2015.

[Coo18] J. Cook, *Properties of eigenvalues on Riemann surfaces with large symmetry groups*, PhD thesis, Loughborough University, arXiv:2108.11825, 2018.

[CP23] G. Cornelissen and N. Peyerimhoff, *Twisted isospectrality, homological wideness, and isometry—a sample of algebraic methods in isospectrality*, SpringerBriefs in Mathematics, Springer, Cham, [2023] ©2023.

[ECH+92] D. B. A. Epstein, J. W. Cannon, D. F. Holt, S. V. F. Levy, M. S. Paterson, and W. P. Thurston, *Word processing in groups*, Jones and Bartlett Publishers, Boston, MA, 1992. MR 1161694

[EH00] D. B. A. Epstein and D. F. Holt, *Efficient computation in word-hyperbolic groups*, Computational and geometric aspects of modern algebra (Edinburgh, 1998), London Math. Soc. Lecture Note Ser., vol. 275, Cambridge Univ. Press, Cambridge, 2000, pp. 66–77.

[FBP23a] M. Fortier Bourque and B. Petri, *The Klein quartic maximizes the multiplicity of the first positive eigenvalue of the Laplacian*, to appear in Journal of Differential Geometry, arXiv:2111.1469, 2023+.

[FBP23b] ———, *Linear programming bounds for hyperbolic surfaces*, preprint, arXiv:2302.02540, 2023.

[GAP22] The GAP Group, *GAP – Groups, Algorithms, and Programming, Version 4.12.2*, 2022.

[GPSDX23] E. Gesteau, S. Pal, D. Simmons-Duffin, and Y. Xu, *Bounds on spectral gaps of hyperbolic spin surfaces*, preprint, arXiv:2311.13330, 2023.

[Hea90] P. J. Heawood, *Map colouring theorems*, Quarterly J. Math. **24** (1890), 363–388.

[Hec12] F. Hecht, *New development in FreeFEM++*, J. Numer. Math. **20** (2012), no. 3-4, 251–265. MR 3043640

[Hej76] D. A. Hejhal, *The Selberg trace formula for* $\mathrm{PSL}(2, R)$. *Vol. I*, Lecture Notes in Mathematics, vol. Vol. 548, Springer-Verlag, Berlin-New York, 1976. MR 439755

[HW94] C. D. Hodgson and J. R. Weeks, *Symmetries, isometries and length spectra of closed hyperbolic three-manifolds*, Experiment. Math. **3** (1994), no. 4, 261–274.

[Jen81] F. Jenni, *Ueber das spektrum des Laplace-operators auf einer schar konmpakter Riemannscher flächen*, PhD thesis, University of Basel, 1981.

[Joh17] F. Johansson, *Arb: efficient arbitrary-precision midpoint-radius interval arithmetic*, IEEE Transactions on Computers **66** (2017), 1281–1292.

[Lee23] C.-h. Lee, *Spectrum of the Laplacian on the Fricke–Macbeath surface*, preprint, arXiv:2311.02632, 2023.

[LL21] F. Lin and M. Lipnowski, *Closed geodesics and Frøyshov invariants of hyperbolic three-manifolds*, preprint, arXiv:2105.04675, 2021.

[LL22a] F. Lin and M. Lipnowski, *Monopole Floer homology, eigenform multiplicities, and the Seifert-Weber dodecahedral space*, Int. Math. Res. Not. IMRN (2022), no. 9, 6540–6560.

[LL22b] ———, *The Seiberg-Witten equations and the length spectrum of hyperbolic three-manifolds*, J. Amer. Math. Soc. **35** (2022), no. 1, 233–293.

[LM23] C. Letrouit and S. Machado, *Maximal multiplicity of laplacian eigenvalues in negatively curved surfaces*, preprint, arXiv:2307.06646, 2023.

[Nad87] N. S. Nadirashvili, *Multiple eigenvalues of the Laplace operator*, Mat. Sb. (N.S.) **133(175)** (1987), no. 2, 223–237, 272.

[Pfe08] M. Pfeiffer, *Automata and growth functions for the triangle groups*, PhD thesis, RWTH Aachen University, 2008.

[RY68] G. Ringel and J. W. T. Youngs, *Solution of the Heawood map-coloring problem*, Proc. Nat. Acad. Sci. U.S.A. **60** (1968), 438–445.

[Ser77] J.-P. Serre, *Linear representations of finite groups*, Graduate Texts in Mathematics, Vol. 42, Springer-Verlag, New York-Heidelberg, 1977, Translated from the second French edition by Leonard L. Scott.

[Sév02] B. Sévennec, *Multiplicity of the second Schrödinger eigenvalue on closed surfaces*, Math. Ann. **324** (2002), no. 1, 195–211. MR 1931764

[The21] The Sage Developers, *Sagemath, the Sage Mathematics Software System (Version 9.3)*, 2021, https://www.sagemath.org.

Appendix A. Character tables

In this appendix, we present the character tables of the isometry groups G_{10} and G_{17} of X_{10} and X_{17}. These were produced with the interface to `GAP` of `SageMath`. These tables list the irreducible characters over $\mathbb{C}$. We use [Ser77, Proposition 39] to determine whether the corresponding irreps are realizable over $\mathbb{R}$ or not. These computations can be found in the `Jupyter` notebooks `verify_genus_10` and `verify_genus_17`.

	$\{e\}$	C_1	C_2	C_3	C_4	C_5	C_6	C_7	C_8	C_9	C_{10}
χ_1	1	1	1	1	1	1	1	1	1	1	1
χ_2	1	-1	1	1	1	1	-1	-1	1	1	-1
χ_3	2	0	-1	2	2	2	0	0	-1	-1	0
χ_4	2	0	-1	0	-2	2	$-\zeta_8-\zeta_8^3$	0	1	-1	$\zeta_8+\zeta_8^3$
χ_5	2	0	-1	0	-2	2	$\zeta_8+\zeta_8^3$	0	1	-1	$-\zeta_8-\zeta_8^3$
χ_6	3	-1	0	-1	3	3	1	-1	0	0	1
χ_7	3	1	0	-1	3	3	-1	1	0	0	-1
χ_8	4	0	1	0	-4	4	0	0	-1	1	0
χ_9	8	-2	2	0	0	-1	0	1	0	-1	0
χ_{10}	8	2	2	0	0	-1	0	-1	0	-1	0
χ_{11}	16	0	-2	0	0	-2	0	0	0	1	0

Table 1. The character table of G_{10}. In this table, $\zeta_8 = e^{i\pi/4}$. The columns correspond to conjugacy classes and the rows to irreducible characters. χ_4 and χ_5 are not realizable over $\mathbb{R}$ and give rise to real irreps of twice their complex dimension. All the other irreps are realizable over $\mathbb{R}$.

	$\{e\}$	C_1	C_2	C_3	C_4	C_5	C_6	C_7	C_8	C_9	C_{10}
χ_1	1	1	1	1	1	1	1	1	1	1	1
χ_2	3	3	-1	-1	-1	1	0	0	$\zeta_7^3+\zeta_7^5+\zeta_7^6$	$\zeta_7+\zeta_7^2+\zeta_7^4$	1
χ_3	3	3	-1	-1	-1	1	0	0	$\zeta_7+\zeta_7^2+\zeta_7^4$	$\zeta_7^3+\zeta_7^5+\zeta_7^6$	1
χ_4	6	6	2	2	2	0	0	0	-1	-1	0
χ_5	7	7	-1	-1	-1	-1	1	1	0	0	-1
χ_6	7	-1	3	-1	-1	1	1	-1	0	0	-1
χ_7	7	-1	-1	-1	3	-1	1	-1	0	0	1
χ_8	8	8	0	0	0	0	-1	-1	1	1	0
χ_9	14	-2	2	-2	2	0	-1	1	0	0	0
χ_{10}	21	-3	1	1	-3	-1	0	0	0	0	1
χ_{11}	21	-3	-3	1	1	1	0	0	0	0	-1

Table 2. The character table of G_{17}. In this table, $\zeta_7 = e^{2i\pi/7}$. χ_2 and χ_3 are not realizable over $\mathbb{R}$ and give rise to real irreps of twice their complex dimension. All the other irreps are realizable over $\mathbb{R}$.

Département de mathématiques et de statistique, Université de Montréal, 2920, chemin de la Tour, Montréal (QC), H3T 1J4, Canada

Email address: maxime.fortier.bourque@umontreal.ca

Département de mathématiques et de statistique, Université de Montréal, 2920, chemin de la Tour, Montréal (QC), H3T 1J4, Canada

Email address: emile.gruda-mediavilla@umontreal.ca

Institut de Mathématiques de Jussieu–Paris Rive Gauche and Institut universitaire de France ; Sorbonne Université and Université Paris Cité, CNRS, IMJ-PRG, F-75005 Paris, France;

Email address: bram.petri@imj-prg.fr

Département de mathématiques et de statistique, Université de Montréal, 2920, chemin de la Tour, Montréal (QC), H3T 1J4, Canada

Email address: mathieu.pineault.1@umontreal.ca